18TH WORLD CONFERENCE ON EARTHQUAKE ENGINEERING
WCEE2024
MILAN

MILAN, ITALY
30TH JUNE - 5TH JULY 2024

www.wcee2024.it

CFS-NHERI 10-STORY BUILDING SHAKE TABLE TEST SPECIMEN: DESIGN UPDATES

A. Singh[1], J. Zhang[2], D. Rivera[2], M. Eladly[1], H. Jones[3], A. Kovac[4], L. Padgett[5], D. Rivera[6,7], K. Smith[4], S. Torabian[1], K. D. Peterman[8], B. W. Schafer[1] & T. C. Hutchinson[2]

[1] Department of Civil and Systems Engineering, Johns Hopkins University, Baltimore, USA, amanprs@jhu.edu

[2] Department of Structural Engineering, University of California San Diego, La Jolla, USA

[3] DCI Engineers, Denver, USA

[4] Construction Specialties, Muncy, USA

[5] ClarkDietrich Engineering Services, Warren, USA

[6] Superior Wall Systems, Fullerton, USA

[7] MID-RISE Modular, Los Angeles, USA

[8] Department of Civil and Environmental Engineering, University of Massachusetts Amherst, Amherst, USA

Abstract: *Cold-formed steel (CFS) framing offers many benefits to buildings in seismically active regions. The light weight and ductility offered by a CFS-framed structure aligns with system resiliency needs in moderate to high seismic zones. Additionally, the seismic resistance of such repetitively framed structures is unique due to large overstrength and the significant contribution of non-designated systems in the lateral response. However, the use of CFS framing for construction of mid to high-rise structures in the North American construction industry is severely restricted due to a lack of available full-scale system level test data documenting both earthquake and post-earthquake fire response. To fully utilize this form of construction and meet the growing needs of urban housing needs, a 10-story CFS-framed building, herein referred to as the CFS-NHERI 10-story building, is planned to be tested under increasing earthquake motion intensity, followed by live fire testing. The building will have a floor plan of 11.0 m×6.9 m and a consistent 3.05 m story height, and will be tested at the NHERI 6-DOF Large High-Performance Outdoor Shake Table (LHPOST6) facility at University of California, San Diego. This paper builds on an earlier design narrative, documenting the structural design and detailing advances to the test specimen, with specific focus on floor and roof diaphragm updates to embrace a modular stair system within the floor plan of the building. The stairs will ensure safe egress in and out of a building, even after a maximum considered earthquake scaled test, adopting seismically resilient connections facilitated by releases at landing levels. In addition, this paper presents the transfer plate design detailed for adapting the lateral force resisting system and stairs assembly to the unique attachment conditions of the shake table platen, as well as an innovation recently supported in the construction of the specimen, namely embracing modular building features.*

1. Introduction

Buildings utilizing lightweight cold-formed steel (CFS) framing are a growing class of structures that have seen a significant growth in adoption across the North American construction industry. Owing to features such as low installation and maintenance costs, faster construction through use of prefabricated or modular units, non-combustibility, resistance to moisture damage and near 100% use of recycled steel, the use of CFS-framed building systems is rapidly growing and stands to provide an important part of the solution to housing and basic building infrastructure demands. Additionally, the lightweight steel framing offers high durability and ductility and resists fire spread in case of accidents which aligns with the improved seismic resiliency and post-earthquake fire performance needs in moderate to high seismic zones (Schafer, 2011).

Recent investigations into the system-level performance of CFS-framed buildings by Peterman et al. (2016) and Hutchinson et al. (2021) have also demonstrated their robust structural performance in low-rise buildings under seismic and post-earthquake fire hazard scenarios. The associated projects, referred to as CFS-NEES and CFS-HUD respectively, tested a 2-story and a 6-story CFS-framed building, and highlight the overstrength that manifests courtesy of non-seismic designated and/or architectural finish elements. While these experimental investigations, accompanied by numerical modelling and several component-level experimental efforts, have furthered the understanding of the behaviour of CFS-framed assemblies, certain barriers remain that restrict CFS framing from realizing its full potential for meeting the growing requirements of urban housing needs. Notably, generating full-scale system level test data documenting the performance of mid-rise CFS-framed buildings in response to both earthquake and post-earthquake fire hazards is an important hurdle to overcome.

A multi-university-industry collaborative effort, coined the CFS-NHERI project, intends to advance the knowledge of the seismic performance of mid-rise CFS-framed building systems by testing a 10-story building, herein referred to as the CFS-NHERI test building, under increasing, multi-directional earthquake motion intensity and subsequent live fire testing at the NHERI 6-DOF Large High-Performance Outdoor Shake Table (LHPOST6) facility at University of California, San Diego (esec.ucsd.edu). The test building, shown in Figure 1, was designed to have a building height of 31.6 m (103 ft 9 in), exceeding the height limitation of 19.8 m (65 ft) set by the current ASCE 7-22 (2022) design standard. The design also advances the lateral force resisting system (LFRS) details to provide for the increases in the shear and overturning moment demands due to the increase in building height. The data generated from this experimental program will shed light on the impact of architectural exterior and interior finishes, gravity framing and all other framing that is along the same architectural line on the CFS-framed shear wall system. Another key factor, the higher mode effects, which can significantly influence the structural and nonstructural seismic response of tall buildings, will also be studied for the first time for such repetitively framed structures. The test will also provide a valuable opportunity to examine the evolution of damage of different systems within a building and develop accurate fragility information, which can be used to improve loss and downtime predictions and evaluate the functional recovery performance. The knowledge gained from this experimental effort will be used to support improvements in the seismic design codes ASCE 7-22, ASCE 41-17 (2017) and various CFS framing design standards AISI S100-16 (2020a), AISI S220-20 (2020b), AISI S240-20 (2020c), AISI S310-20 (2020d), and AISI S400-20 (2020e).

This paper builds on an earlier design narrative article, Singh et al. (2022), which documents the structural design and detailing decisions adopted for the gravity and lateral force resisting systems of the CFS-NHERI test building. For brevity, only a summary of the design is provided in the following section. This paper specifically focuses on updates to floor diaphragm design to embrace a modular stair system within the floor plan of the building. The seismically resilient stairs will provide safe egress in and out of the building through the use of a variety of different interstory drift-compatible detailing. Additionally, the test building will also explore a variety of construction methods, namely, conventional stick-framing, panelized (2D), and volumetric (3D) modular construction within one building specimen, allowing a unique opportunity to document and compare the efficiency of each construction method, and any differences in structural performance. This paper also documents the challenges posed by the unique attachment conditions of the LHPOST6 shake table platen and the additional detailing required for adapting the lateral force resisting system and stairs assembly to the table platen.

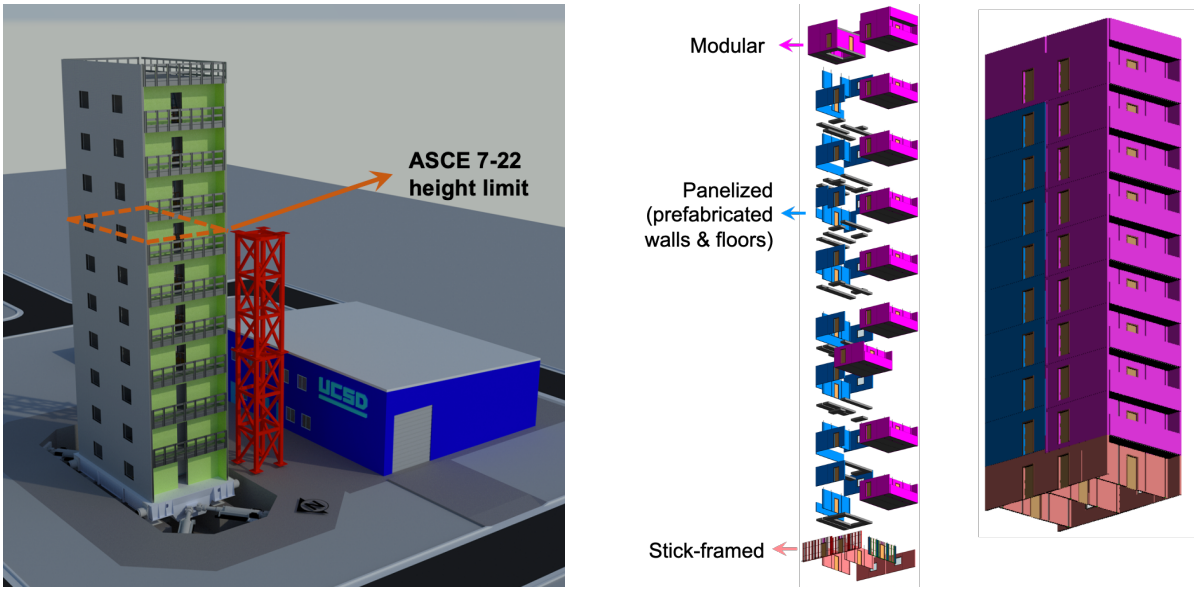

Figure 1. 3D rendering and construction methods planned for the 10-story CFS-NHERI test building.

2. Design summary

2.1. Design criteria

The test building will have a floor plan of 11.6 m×6.9 m (38 ft×22.5 ft) and a consistent 3.05 m (10 ft) story height across ten stories. Together with a 1.1 m (3 ft 9 in) tall parapet, the building will have a total height of 31.6 m (103 ft 9 in). Figure 2 shows the floor plan and a rendering of the test building as assembled at the LHPOST6 facility. The 10-story test building represents a slice of an archetype building (Torabian et al. 2016) at a hypothetical location near Irvine, USA (coordinates: 33.69˚N, -117.83˚W) and site class: C (very dense soil and soft rock) condition. In accordance with ASCE 7-16 (2016), the following design parameters were assumed: risk category: II, spectral acceleration at short periods, S_s = 1.261g, spectral acceleration at a period of 1s, S_1 = 0.452g, and design spectral accelerations, S_{DS} = 1.009g and S_{D1} = 0.452g. The LFRS of the test building consisted of Type I shear walls with single-sided steel sheet sheathing and ledger framing for floor-to-wall connections. The seismic design parameters corresponding to this system were obtained from ASCE 7-16 as: response modification coefficient, R = 6.5, over-strength factor, Ω_o = 3.0 and deflection amplification factor, C_d = 4.0. Fundamental period of building, T_a was estimated based on ASCE 7 Section 12.8.2.1 as 0.632s. The design effective seismic weight, W of the building was estimated as 1575.0 kN (354.1 kips) and the design seismic base shear force, V was calculated as 173.2 kN (38.9 kips) in the two orthogonal directions. The building was also designed for lateral loads from wind with speeds of 100 kmph (63 mph). Sections of building, where fire-testing will be conducted, will have mudded and taped joints per 1-hr fire rated assemblies.

2.2. Lateral force resisting system

As shown in Figure 2, the building uses 152.4 mm (6 in) thick symmetric wall-lines with Type I CFS-framed shear walls on each end with single-sided steel sheet sheathing attached using fasteners. Two 1.83 m (6 ft) long shear walls are placed along each of the longitudinal (east-west) direction wall-lines 1 and 2 (SW2). Similarly, two 1.83 m (6 ft) long shear walls are placed along each transverse (north-south) direction wall-lines C, D and E (SW1 and SW3). Additionally, to incorporate architectural finishes, wall-lines C, D, E and 2 will have fire rated gypsum board finish, typical of interior walls. Wall-line 1 was designed as an exterior wall and will have exterior insulation finishing system (EIFS). It should be noted that the shear walls in the two orthogonal directions incorporate different tie-down detailing systems to represent the possible options reflecting regional preferences. The shear walls along lines C, D and E employ tension tie-rods sandwiched between compression chord stud packs, while shear walls along lines 1 and 2 employ hold-downs attached to stud packs. However, shear walls along longitudinal direction in stories 1-5 are detailed to resist much larger lateral forces. To develop the strengths needed to resist high overturning moment demands, chord studs are designed as hot-rolled steel HSS sections rather than as stud packs. Additionally, welded or bolted plate hold-downs are used in shear walls in stories 2-7 to resist high axial demands. The HSS steel column at level 1 will be directly welded to the transfer plate. Figure 3 shows the different tie-down details used in the shear

walls in the longitudinal direction. The test building will use CFS floor diaphragms with ledger framing for floor-to-wall connections, using 30.5 cm (12 in) deep joists repetitively placed at 40.6 cm (16 in) spacing spanning north-south direction. The floor joists within the panelized diaphragms will have a 19 mm (¾ in) thick cement panel fastened on top, as shown in Figure 4, and a 16 mm (⅝ in) thick gypsum board at the bottom. Similarly, the modules will also employ 30.5 cm deep floor joists at 40.6 cm spacing with a 19 mm thick cement panel fastened on top. However, in addition, the modules will employ 10.2 cm (4 in) deep ceiling joists at 61.0 cm (24 in) spacing spanning east-west direction with a 16 mm thick gypsum board fastened at the bottom.

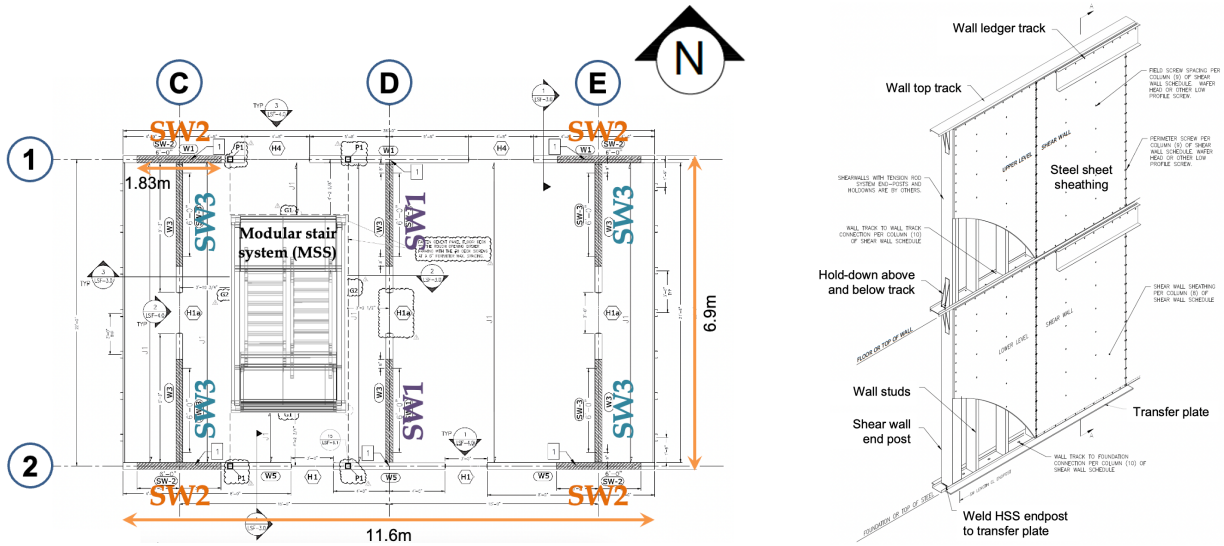

Figure 2. Typical floor plan and steel sheet sheathed shear wall detailing.

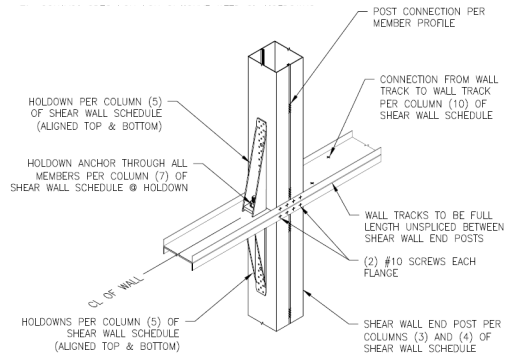

(a) Hold-down attached to built-up chord studs

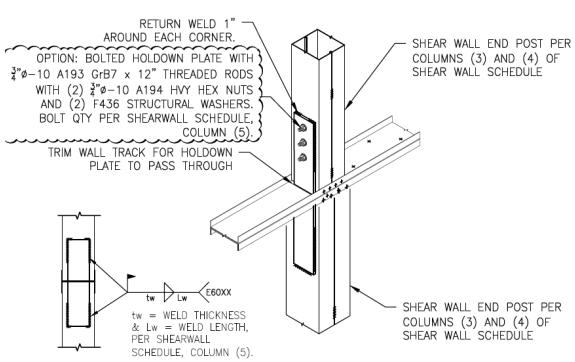

(b) Plate hold-down bolted or welded to built-up chord studs

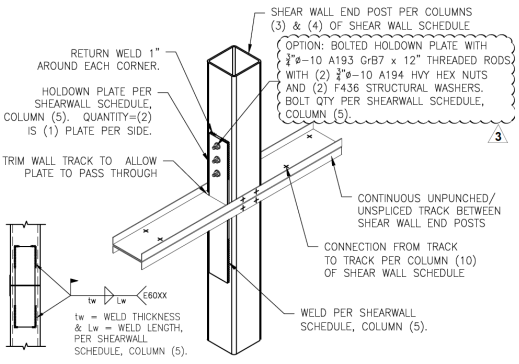

(c) Plate hold-down bolted or welded to HSS column

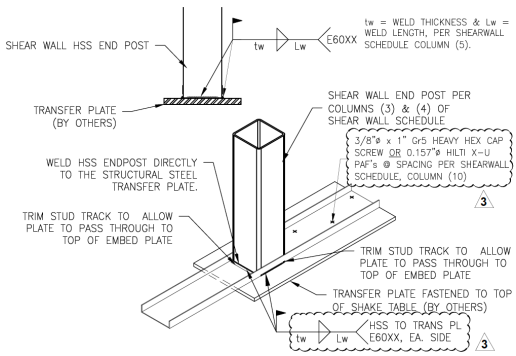

(d) HSS column directly welded to transfer plate

Figure 3. Tie-down systems used in shear wall SW2 at different levels.

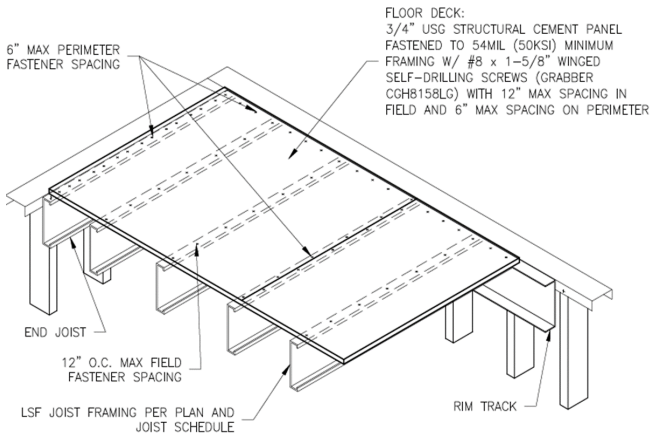

Figure 4. Typical diaphragm detailing and connection to wall framing.

3. Modular stair system (MSS)

As shown in Figure 2, the typical floor diaphragm is provided with a rough opening of size 2.4 m×4.1 m (7.8 ft×13.6 ft) in the west room of the building. These openings are provided to incorporate a self-supporting modular stair system within the floor plan providing egress/ingress to levels 1-9 of the building. The roof diaphragm is provided with an opening of size 1.22 m×1.22 m (4 ft×4 ft) in the west room to provide access to the roof using a fixed ships ladder stair system through an access hatch. Figure 5 provides an elevation and isometric view of the stair system as well as the various handrail and drift-compatible detailing adopted at different floors in the building.

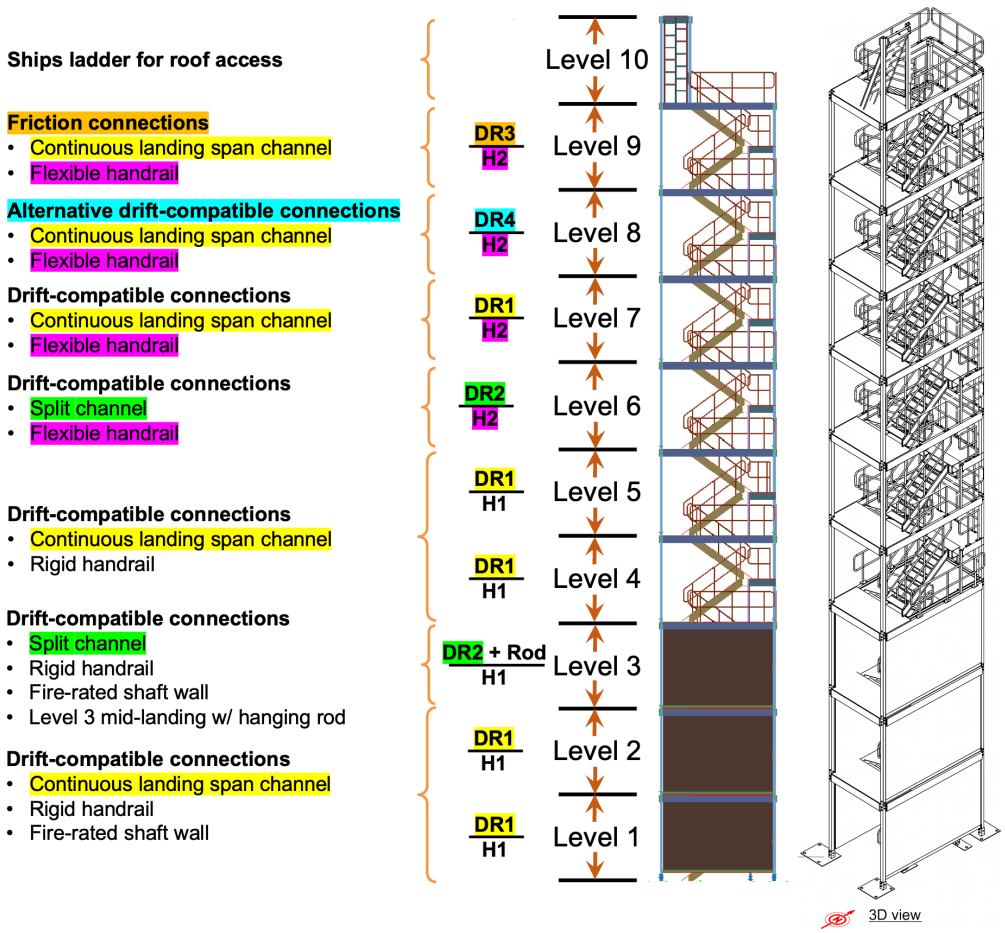

Figure 5. Isometric and elevation view of resilient stair system showing the handrail and drift-compatible detailing variations at different floors planned for the test building.

To support force transfer around diaphragm openings, additional framing in the form of back-to-back girders in the joist span direction (north-south) and rim girder in the east-west direction are provided, as shown in Figure 6. The built-up girders are supported by a CFS post on wall-lines 1 and 2 to transfer the gravity load. The perimeter channels of the stair module are connected to the built-up girders using flat straps with fasteners. The flat straps are designed for inertial forces transferred into the diaphragm due to the stair system weight as per ASCE 7-22 Equation 13.3-1, shown in Eq. (1). The modular stair unit on a typical floor in the test building has a weight of 17.4 kN (3.9 kips), which includes the additional safety guardrails around mid-landing and floor-level opening. The bottom three floors of the stair system are provided with fire-rated shaft walls, which increase the weight of the stair unit to 28.9 kN (6.5 kips). The ships ladder at Level 10 for accessing the roof weighs approximately 5.0 kN (1.1 kips).

$$F_p = 0.4 S_{DS} I_p W_p \left[\frac{H_f}{R_\mu}\right]\left[\frac{C_{AR}}{R_{po}}\right] \quad (1)$$

Where importance factor, I_p = 1.5, as the stair system provides essential egress; W_p is the tributary weight of the stairs at each floor; structure ductility reduction factor, R_μ = 1.3; component resonance ductility factor, C_{AR} = 2.2; and component strength factor, R_{po} = 1.5 for egress stairs as per ASCE 7-22 Table 13.5-1. A factor for amplification with height, H_f is determined as per ASCE 7-22 Equation 13.3-4, shown in Eq. (2).

$$H_f = 1 + a_1\left(\frac{z}{h}\right) + a_2\left(\frac{z}{h}\right)^{10} \quad (2)$$

Where a_1 and a_2 are factors calculated using code-based estimate of building fundamental period, T_a = 0.632s. The maximum design demand for flat straps was calculated as 27.8 kN (6.2 kips) and were designed to keep their demand to capacity utilization ratio under 0.5, thereby providing a factor of safety for this critical connection in the egress system.

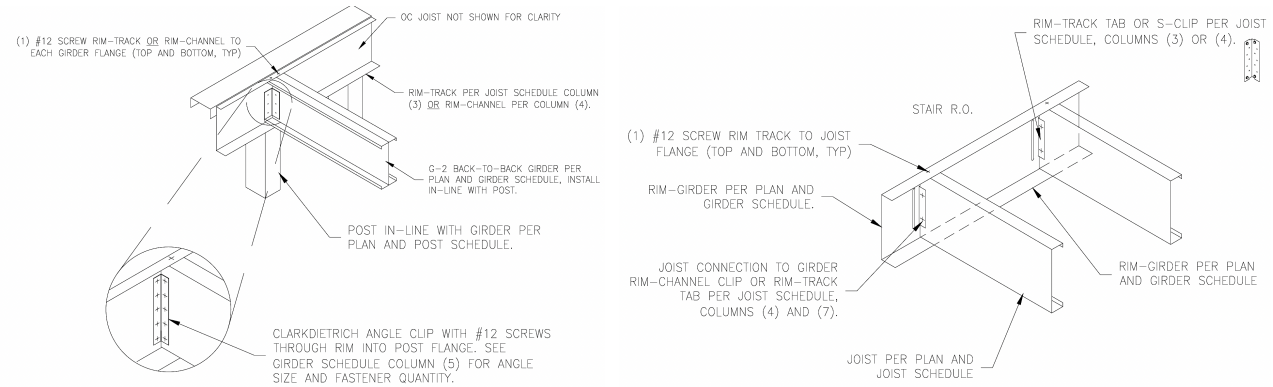

Figure 6. Framing details for force transfer around openings.

It should be noted that the introduction of a concentrated weight in the form of stairs in the west room causes an eccentricity by moving the center of mass of the floor. It also increases the diaphragm shear within the tributary area of shear walls on line C and D. On levels 4-10, this is rectified by leveraging the higher weight of the east room module and strategically placing supplemental weight across the floor plan such that the eccentricity becomes negligible and floor design weight remains unchanged. On levels 1-3, this solution, by itself, is not sufficient due to higher stair weight with inclusion of fire-rated shaft walls. As a result, shear walls SW3 on line C are designed for 13% higher shear demand, compared to shear demand before the modular stair system was introduced within the floor plan of the building. However, to keep the center of rigidity unchanged and not introduce torsion, shear walls SW3 on line E on levels 1-3 are also designed for 13% higher shear demand. Additionally, supplemental weight is strategically placed in the east balcony area such that the eccentricity becomes negligible and floor design weight remains unchanged.

As shown in Figure 5, a variety of friction/slotted and drift-release connections (DR1-DR4) will be used to accommodate the interstory drift at each floor. It should be noted that the mid-landing for level 3 will be hung using rods instead of the typical detail where mid-landings for the stairs are supported on HSS columns. DR1 and DR2 are drift-release connections developed by industry partners and their performance within a stairs system was recently evaluated through shake table testing of a 10-story mass timber rocking wall structure

(Sorosh et al. 2022). These two details differ only in terms of the channel that houses and is attached to the connection, i.e., a continuous channel vs. split channel, as shown in Figure 7. A friction connection DR3 and another drift-release connection DR4 are newly developed ideas proposed by Sorosh et al. (2024a) and Construction Specialties, respectively, which will also be employed with the CFS-NHERI test building. Two types of handrails with rigid (H1) or flexible (H2) connections will be tested, as their damage has been noted even in resilient stairs in recent tests (Sorosh et al. 2024b), in conjunction with the variations of drift-release connections at different floors as shown in Figure 5.

(a) (b) (c)

Figure 7. Various stair landing-flight connection details: (a) drift-release connection with a (b) continuous channel (DR1), and (c) split channel (DR2) (Sorosh et al. 2024b).

4. Connection to shake table platen through transfer plates

The floor plan of the test building, as assembled at the LHPOST6 facility, overlaid on the shake table platen hole pattern is shown in Figure 8(a). The platen has a uniform 0.6 m×0.6 m (2 ft×2 ft) on center grid pattern over its 12.2 m×7.6 m (40 ft×25 ft) footprint. However, it should be noted that the holes have different attachment conditions due to the structural configuration of the platen support, namely with a trapezoidal cross-section resulting in both through and blind holes for attachment. In Figure 9, specifically, 1.2 m (4 ft) or 2.1 m (7 ft) long through holes are denoted by white circles, and fine-threaded blind holes are denoted by grey circles. The building floor plan occupies almost the entire area of the table platen. Figure 8(a) also shows the locations of the tension tie-rods on wall-lines C, D and E and HSS columns on wall-lines 1 and 2 with respect to the shake table holes. The bottom track of all wall-lines will bear on a 51 mm (2 in) thick A572 Gr50 (ASTM 2021) steel transfer plates, as shown in Figure 9, and connected using power-actuated heavy-duty fasteners.

Since, the HSS columns for shear walls in longitudinal direction are located approximately in the middle of four table holes, the transfer plate at all shear wall ends on wall-lines 1 and 2 are post-tensioned to the shake table using ϕ46 mm (ϕ1-3/4 in) Dywidag bars. This is shown using green circles in Figure 8(b). Tension tie-rods for shear walls on wall-lines C and E are collocated at the same location as a hole on the shake table platen. This allows the tension tie-rod to be attached directly to the post-tensioned Dywidag bar using a coupler. However, tension tie-rods for shear walls on wall-line D lie in between two table platen holes. Therefore, the axial tension force from the tie-rods must be spread across and transferred to the post-tensioned Dywidag bars. This is achieved through an HSS stub column and plate assembly, details shown in Figure 9. The locations of Dywidag bars used for transferring tie-rod forces are shown using blue squares in Figure 8(b). To transfer the small shear force at the base of the stairs, the modular stair assembly is provided with 12.7 mm (1/2 in) thick A36 (ASTM 2019) steel transfer plates, which will be wrench tightened to the shake table platen using ϕ35 mm (ϕ1-3/8 in) Dywidag bars at locations shown using orange diamonds in Figure 8(b). Purple hexagons within Figure 8(b) show the locations of additional wrench tightened Dywidag bar connections provided to transfer building base shear force into the table platen. In total, the test building including its modular stair system will be connected at 110 locations to the shake table platen.

Prestress force in Dywidag bars is determined based on (a) HSS column and tension tie-rod design forces and (b) attachment condition (through or threaded hole). Threaded holes have greater prestress losses and require additional length above the table platen level to control and develop the prestressing force. Based on these requirements, the prestress forces for post-tensioned bars along wall-line D were determined as 667.2 kN (150 kips), 13% above the required 592.0 kN (133.1 kips) design force per attachment location. Additionally, short HSS columns are used along wall-line D for providing additional length above the table platen, since half the attachment locations have threaded hole configuration. Similarly, the prestress forces for

post-tensioned bars along wall-line C, E were determined as 889.6 kN (200 kips), the amplitude selected to align with the required design force. Attachment locations with threaded hole configuration along these wall-lines also use short HSS columns. Prestress forces for post-tensioned bars along wall-lines 1 and 2 were determined as 889.6 kN (200 kips), 138% above the required 373.2 kN (84 kips) design force per attachment location. Even though the attachment locations along these wall-lines have threaded hole configuration, they were intentionally not provided with additional hardware for prestressing. Instead, allowing for prestress losses, which are estimated to be approximately 30%, was deemed an efficient and simpler solution. The additional details required for complete shear and axial load transfer at the shake table platen are provided in Figure 9.

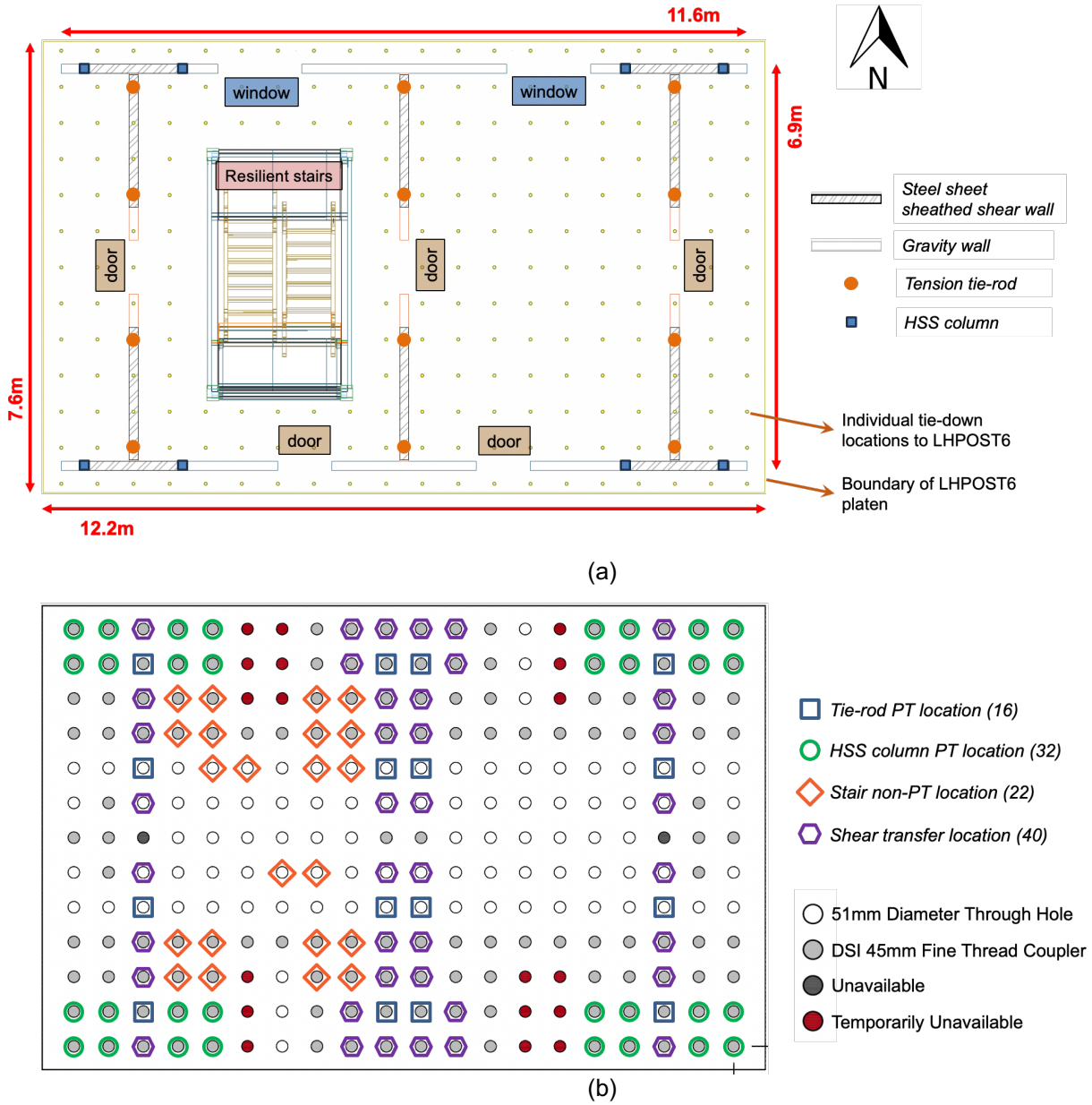

Figure 8. (a) Floor plan of test building overlaid on shake table platen, and (b) shake table platen holes employed for connection by test building and their attachment conditions.

5. Roadmap of near-term activities

5.1. Overview

The 10-story building shake table tests, the capstone effort within the CFS-NHERI project, provides a unique opportunity to characterize the behavior of a state-of-the-art design CFS-framed building under multi-directional seismic input. These tests will improve our understanding regarding the impact of architectural

finishes, non-designated systems, such as gravity walls or window/door framing. The effect on building response due to the addition of a modular stair system with various drift-compatible connections and handrail configurations, and the opening within the floor/roof diaphragms to accommodate the resilient stairs will also be studied. This paper builds upon an earlier design narrative (Singh et al., 2022) providing updates to the floor and roof diaphragm framing to accommodate the modular stair system within the floor plan of the building. In addition, the design and detailing required to transfer shear and axial loads imposed on the shake table platen by the wall bracing and modular stairs assembly are also documented in this paper.

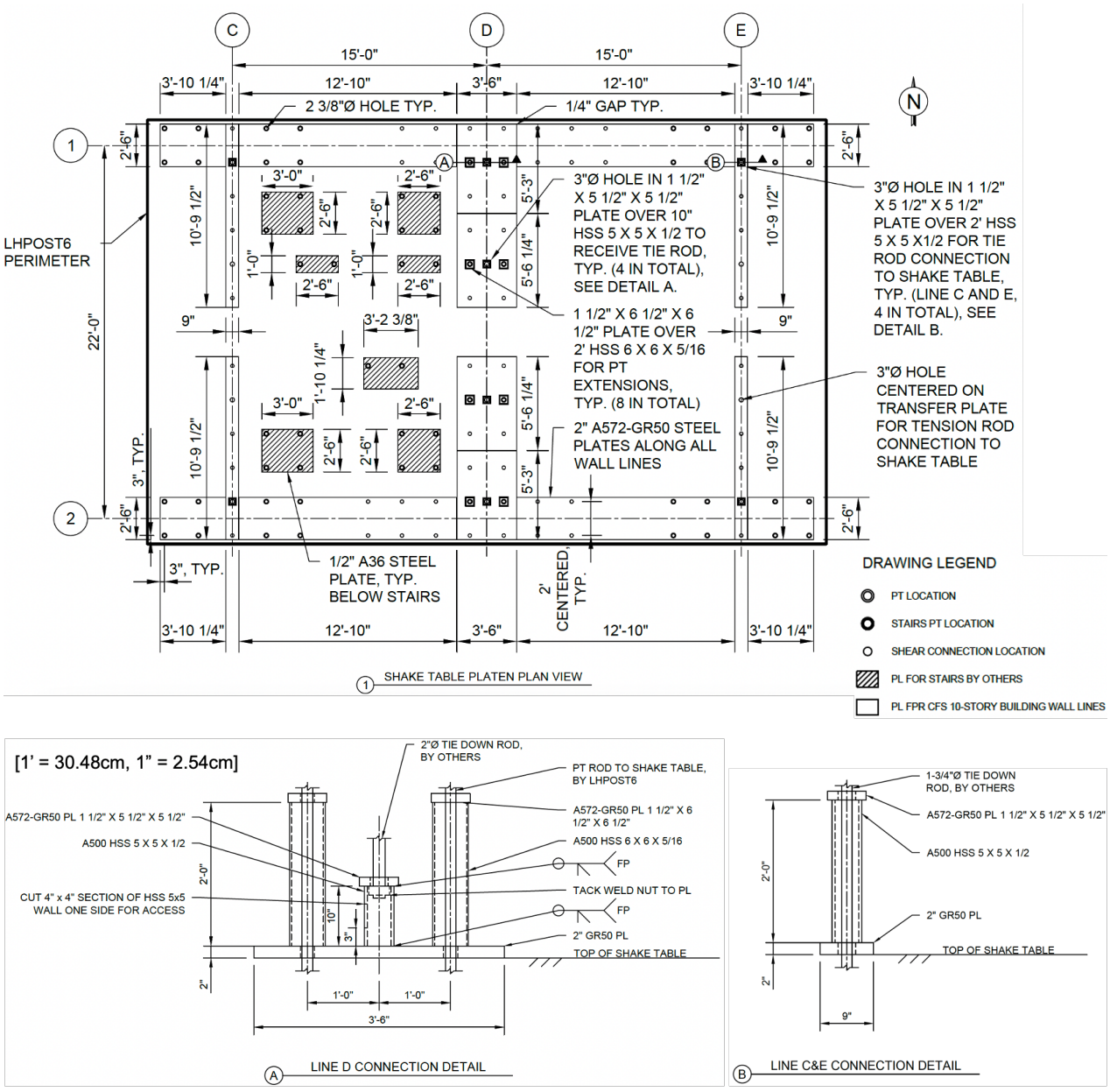

Figure 9. Transfer plate details under wall-lines and stairs system.

5.2. Next steps

Near-term activities to be undertaken in the planning of the CFS-NHERI 10-story building experiments include the following: 1) design of modular volumetric units to be installed within the upper five-levels of the test specimen, 2) development of a test protocol and instrumentation plans to be executed during the testing, and 3) development of material takeoffs and procurement/delivery plans, and preparation of shop drawings for construction. Subsequently, construction is slated to commence at the LHPOST6 facility (at the time of preparation of this paper) in July 2024. Note that a test protocol consisting of a sequence of earthquake motions imposed with increasing hazard-scaled intensity (e.g. service-level, 50% design, design and maximum

credible earthquake levels), which progressively damages the test specimen, such as the on-the-fly motion scaling parameter adjustment methodology developed by Wang et al. (2024), will be adopted for the test program. This development will be supported by ground motion selection and scaling based on chosen design location (Zhang et al. 2024a) as well as predictions of the test building seismic behavior through pre-test numerical modeling efforts (Zhang et al. 2022, 2024b). The building specimen will be densely instrumented to capture accelerations, forces, and displacements, with more than 700 sensors. Sensors will be installed at various locations throughout the building to capture critical engineering demand parameters for nonstructural components of interest to understand the system resiliency. The shake table tests also provide an opportunity to determine measurement accuracy and reliability of alternative sensing techniques on real structures subjected to severe shaking, such as laser-based optical sensing (Petrone et al. 2023) and vision-based sensing using camera-equipped unmanned aerial vehicles (UAVs) (Wang et al. 2022, Cao et al. 2024). In addition, digital still, 360° panoramic/virtual reality media and video imagery will be captured throughout construction, testing and de-erection.

Finally, embracing modular construction within this specimen offers several benefits such as lower material waste, lower carbon footprint and embodied carbon, and greater energy efficiency through tighter building envelopes. However, to modularize portions of the test building, a creative solution is engineered to meet the module strength and stiffness needs for handling-induced damage-free transportation without significantly increasing the seismic weight of a fundamentally light-framed system. This experimental program offers an exciting opportunity for collaboration between researchers and industry partners to bring forth new ideas to realize modular construction within CFS framing systems. The CFS-NHERI capstone experiment program will generate valuable knowledge which accrues benefits not just for CFS-framed systems, but all systems, through improvements in design standards and construction handbooks.

6. Acknowledgments

The research presented is funded through the National Science Foundation (NSF) grants CMMI 1663569 and CMMI 1663348, project entitled: Collaborative Research: Seismic Resiliency of Repetitively Framed Mid-Rise Cold-Formed Steel Buildings. Complementary post-earthquake live fire testing is being undertaken by Dr. Richard Emberley at California Polytechnic State University, San Luis Obispo, USA with the support of the California Seismic Safety Commission and California Governor's Office of Emergency Services agreement A211006635. The newly supported task of integrating modular volumetric construction concepts is supported through the Department of Housing and Urban Development, instrument no. RP-22-CA-005. Support for the second author from UC San Diego Department of Structural Engineering Distinguished Fellowship is greatly appreciated. Contributions of the NHERI LHPOST6 facility operations manager Dr. Koorosh Lotfizadeh, site staff Alex Sherman and Abdullah Hamid in the test program planning are greatly appreciated. Findings, opinions, and conclusions are those of the authors and do not necessarily reflect those of the sponsoring organizations.

7. References

AISI (2020a). *AISI S100-16. North American Specification for the Design of Cold-Formed Steel Structural Members*, American Iron and Steel Institute, Washington DC, USA.

AISI (2020b). *AISI S220-20. North American Standard for Cold-Formed Steel Nonstructural Framing*, American Iron and Steel Institute, Washington DC, USA.

AISI (2020c). *AISI S240-20. North American Standard for Cold-Formed Steel Structural Framing*, American Iron and Steel Institute, Washington DC, USA.

AISI (2020d). *AISI S310-20. North American Standard for the Design of Profiled Steel Diaphragm Panels*, American Iron and Steel Institute, Washington DC, USA.

AISI (2020e). *AISI S400-20. North American standard for seismic design of cold-formed steel structural systems*, American Iron and Steel Institute, Washington DC, USA.

ASCE/SEI (2016). *ASCE/SEI 7-16. Minimum design loads for buildings and other structures*, American Society for Civil Engineers, Reston, USA.

ASCE/SEI (2017). *ASCE/SEI 41-17. Seismic evaluation and retrofit of existing buildings*, American Society for Civil Engineers, Reston, USA.

ASCE/SEI (2022). *ASCE/SEI 7-22. Minimum design loads for buildings and other structures*, American Society for Civil Engineers, Reston, USA.

ASTM (2019). *ASTM A36/A36M-19. Standard Specification for Carbon Structural Steel*, American Society for Testing and Materials, West Conshohocken, USA.

ASTM (2021). *ASTM A572/A572M-21. Standard Specification for High-Strength Low-Alloy Columbium-Vanadium Structural Steel*, American Society for Testing and Materials, West Conshohocken, USA.

Cao P., Ji R., Ma Z., Sorosh S., Lo E., Norton T., Driscoll J., Wang X., Hutchinson T., Pei S., Kuester F. (2024). "UAV-based video analysis and semantic segmentation for SHM of earthquake-excited structures", *Proceedings of the 18th World Conference on Earthquake Engineering*, Milan, Italy.

Petrone F., Perez R., Coates J., McCallen D. (2023). A Biaxial Discrete Diode Position Sensor for Rapid Postevent Structural Damage Assessment, *Journal of Structural Engineering*, *149*(3), p.04022251. DOI: 10.1061/JSENDH.STENG-11776.

Hutchinson T.C., Wang X., Hegemier G., Kamath P., Meacham, B. (2021). Earthquake and postearthquake fire testing of a midrise cold-formed steel-framed building. I: Building response and physical damage, *Journal of Structural Engineering*, *147*(9), p.04021125. DOI: 10.1061/(ASCE)ST.1943-541X.0003097

Peterman K.D., Stehman M.J., Madsen R.L., Buonopane S.G., Nakata N., Schafer, B.W. (2016). Experimental seismic response of a full-scale cold-formed steel-framed building. I: System-level response, *Journal of Structural Engineering*, *142*(12), p.04016127. DOI: 10.1061/(ASCE)ST.1943-541X.0001577.

Schafer B.W. (2011). Cold-formed steel structures around the world: A review of recent advances in applications, analysis and design, *Steel Construction*, *4*(3), pp.141-149. DOI: 10.1002/stco.201110019.

Singh A., Hutchinson T.C., Torabian S., Schafer B.W., Peterman K.D., Padgett L., Jones, H. (2022). "Structural design narrative of the CFS-NHERI 10-story test building for multi-dimensional shake table testing", *Proceedings of the Cold-Formed Steel Research Consortium (CFSRC) Colloquium 2022*, Baltimore, USA.

Sorosh S., Hutchinson T.C., Ryan K.L. (2022). "NHERI TallWood 10-story test nonstructural, part 4 of 4: prefabricated steel stair subassemblies", *Proceedings of the 12th National Conference on Earthquake Engineering*, Salt Lake City, USA.

Sorosh S., Hutchinson T.C., Smith K., Kovac A. (2024a). "Advancing Resilient Stair Systems Considering Friction-Based Drift-Compatible Connections", *Proceedings of the 18th World Conference on Earthquake Engineering*, Milan, Italy.

Sorosh S., Hutchinson T.C., Ryan K.L., Smith K., Belvin R., Kovac A., Pei S., Dowden D.M. (2024b). "Performance of a 10-story steel stair tower within the NHERI TallWood building", *Proceedings of the 18th World Conference on Earthquake Engineering*, Milan, Italy.

Torabian S., Nia Z., Schafer B. (2016). "An archetype mid-rise building for novel complete cold-formed steel buildings", *Proceedings of International Specialty Conference on Cold-Formed Steel Structures*, Baltimore, USA.

Wang X., Lo E., De Vivo L., Hutchinson T.C., Kuester F. (2022). Monitoring the earthquake response of full‐scale structures using UAV vision-based techniques, *Structural control and health monitoring*, *29*(1), e2862. DOI: 10.1002/stc.2862.

Wang X., Singh A., Hutchinson T.C. (2024). "Development of a shake table motion scaling strategy for seismic performance evaluation", *Proceedings of the 18th World Conference on Earthquake Engineering*, Milan, Italy.

Zhang J., Singh A., Hutchinson T.C., Wang, X. (2022). "Seismic analysis of the 10-Story CFS-NHERI building", *Proceedings of the Cold-Formed Steel Research Consortium (CFSRC) Colloquium 2022*, Baltimore, USA.

Zhang J., Singh A., Eladly M., Marcinek, S., Guha, S., Peterman K.D., Schafer B.W., Hutchinson T.C. (2024a). "Ground motion selection and scaling considerations for the CFS-NHERI capstone 10-story building specimen", *Proceedings of the 18th World Conference on Earthquake Engineering*, Milan, Italy.

Zhang J., Singh A., Eladly M., Schafer B.W., Hutchinson T.C. (2024b). "Pre-test numerical modelling of the CFS-NHERI 10-Story capstone building", *Proceedings of the 18th World Conference on Earthquake Engineering*, Milan, Italy.